Simultaneous observation of the scattered light in the rainbow region of two falling droplets

N. Roth*, G. Gerhardinger, A. Mariani and B. Weigand
Institut für Thermodynamik der Luft- und Raumfahrt, University of Stuttgart, Germany
norbert.roth@uni-stuttgart.de

Abstract

The droplets are falling within a observation chamber and while they are falling they are illuminated by a vertical laser beam. The light scattered in the forward hemisphere is used to determine the droplet size using the interference pattern. The light scattered in the backward hemisphere in the region of the first rainbow is used to obtain the refractive index. The two lenses in front of the two cameras are not used as Fourier lenses anymore. The droplets are first imaged by the lenses and then the image plane of the cameras is moved along the optical axis in order to obtain defocussed images of the droplet. Then interference fringes in the forward direction and the first rainbow in the backward direction become visible. For the forward direction this is a well known method used in the so called ILIDS or IMI technique, which allows to determine the droplet sizes and velocities in a plane of a multiphase flow field. Here, in addition to the scattered light in the forward direction, the position of the rainbows from the light scattered in the backward direction is determined for two droplets of slightly different terminal velocity falling simultaneously within the observation chamber. Examples for two droplets of different substances are shown. In one case the distance between the droplets increases and in the other case a collision of the two droplets is observed.

Introduction

Detailed studies of the dynamical behaviour of droplets are important to obtain insight in basic physical processes occurring for instance during droplet evaporation, droplet collisions, droplet impacts on solid or liquid surfaces. Basic experiments are necessary, which allow to control the boundary conditions very precisely, in order to validate numerical simulations of these processes. Then with the numerical simulations for instance flow fields or pressure fields inside the droplets are obtained, which is very difficult or impossible to be obtained by experiments. In addition numerical simulations allow to vary the governing parameters independently from each other in order to obtain a large data basis. Experiments and numerical simulations together are the basis for the development of models describing droplet dynamics. These models can be implemented in codes, which allow to simulate complex natural or technical systems. The experimental techniques have to be extended and improved in order to take new developments in the numerical sector into account.

Here a technique is presented, which allows to observe two droplets falling freely in an observation chamber. This is a further development of the techniques described in (1; 2). As in these publications droplet parameters like velocity, size and refractive index are obtained from the light scattered by the droplets, which are illuminated with a laser beam. For the size measurements the light scattered in the forward hemisphere is studied (3). Here more than one droplet is observed, therefore an optical arrangement with out of focus imaging is used, as in the so-called ILIDS or IMI technique (4; 5). The refractive index of the droplet is obtained by observing the first rainbow in the backward hemisphere (6). Here again the out of focus technique is used in order to observe two droplets. These techniques are described in the following section.

Experimental Methods

The essential difference to the experimental techniques described e.g. in (2) is that now more than one droplet can be observed simultaneously. First of all the experimental setup is described. A schematic view of this setup is shown in Fig. 1, which is similar to the one used in former experiments.

The droplets are generated by one or two droplet on demand generators and horizontally injected in a transparent observation chamber with a length of $100\,\mathrm{mm}$ and a cross section of approximately $10 \times 10\,\mathrm{mm}^2$. The droplet on demand generators have to be adjusted very precisely, so that the droplets, after their horizontal deceleration, are falling freely downwards in the observation chamber along the illuminating laser beam. In order to avoid vapour accumulation in the observation chamber the chamber is purged by a very low air flow with room temperature.

While the droplets are falling downwards the scattered light is observed in the forward hemisphere by a cylindrical lens and a linear CCD-camera and in the backward hemisphere in the region of the first rainbow by an

*Corresponding author: norbert.roth@uni-stuttgart.de

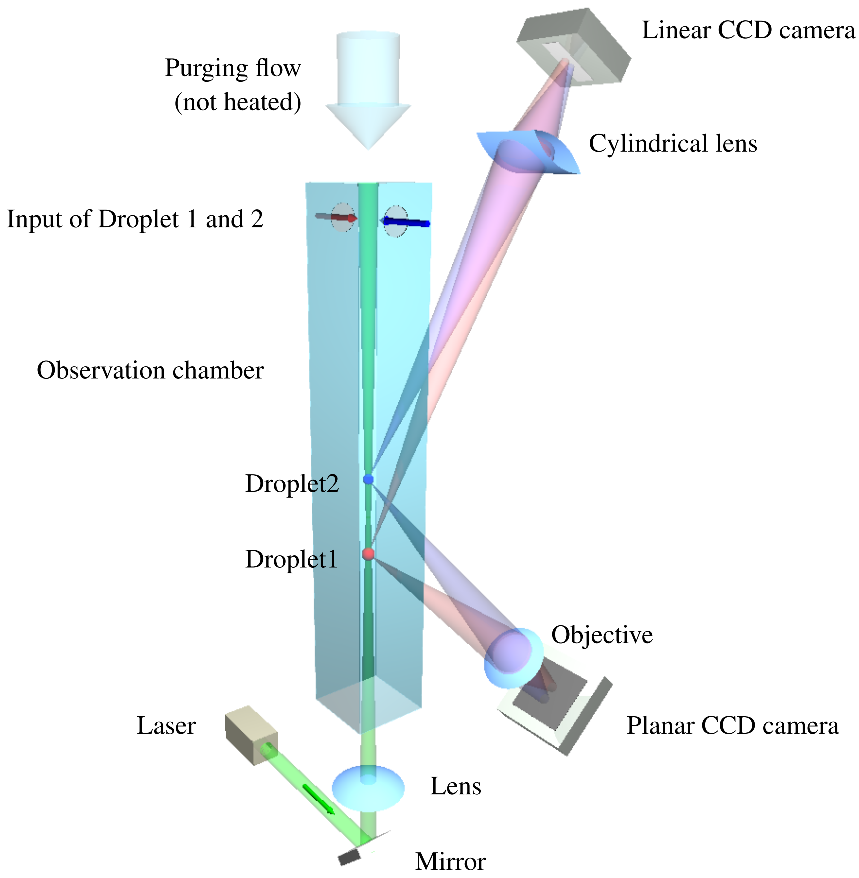

Figure 1: Schematic view of the experimental setup

objective and a planar CCD-camera. There are three basic possibilities of the arrangement of lenses and cameras. In the first one, which has been used e.g. in (1), the camera is located in the focal plane of the lens (Fourier lens). Then the scattered light is independent of the position of the droplet. However, only one single droplet can be observed. In the second one, the droplet is imaged by the lens and the camera. In this case glare points of the droplets are observed and more droplets can be imaged. However, the glare points are very difficult to evaluate. In the third case the camera is moved out of focus until the rays of different scattering order are producing an interference pattern, which can be evaluated.

For the scattered light in the forward hemisphere this leads to the well-known ILIDS or IMI technique for the size measurement. The linear CCD camera detects the light, while the droplet is falling along the observation chamber, with a frequency of $5000\,\mathrm{Hz}$.

For the scattered light in the backwards hemisphere the light in the region of the rainbow is detected by a planar CCD-camera. In order to increase the frequency of the camera up to $60\,\mathrm{Hz}$ not the whole frame of the camera is used. The images consist only of 2048×200 Pixels. An example for one droplet of n-hexadecane is shown in Fig. 2. The red lines, which are parts of a circle line, indicate the aperture of the objective. An experimental correlation is used to evaluate the vertical position of the droplet from the center of the circle. In Fig. 3 the corresponding rainbow signal is shown. This signal has been obtained by a two step processing method for noise filtering. Fifty lines are first summed, and then the signal is smoothed using a sinusoidal weighted averaging algorithm.

While the droplet is falling through the observation chamber the position of the grabbed circle changes and the angle detected by the objective changes too. Therefore the calibration, that means the relation between Pixels on the camera and scattering angle, is changing by the changing position of the droplet (vertical position and distance between droplet and objective). This can be seen from Fig. 4, where a series of images taken by the planar CCD-camera is shown. The red lines, which are part of a circle, indicate again the aperture of the objective. It can be clearly seen that the circles move across the images due to the vertical position of the droplet and that

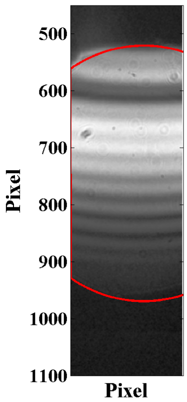

Figure 2: Example of an image of the planar CCD-camera with the scattered light in the rainbow region. The red lines indicate the aperture of the objective and therefore the position of the droplet.

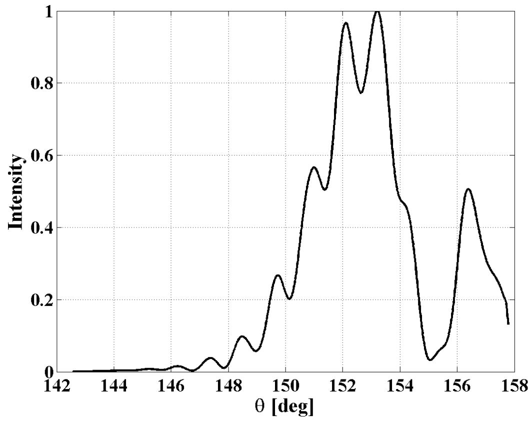

Figure 3: Rainbow signal derived from Fig.2.

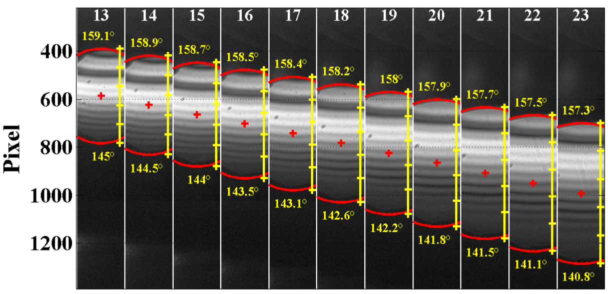

Figure 4: Series of grabbed images of the planar CCD-camera. The red lines indicate the aperture of the objective, the red cross indicates the center of the circle. In yellow the corresponding scattering angles are indicated.

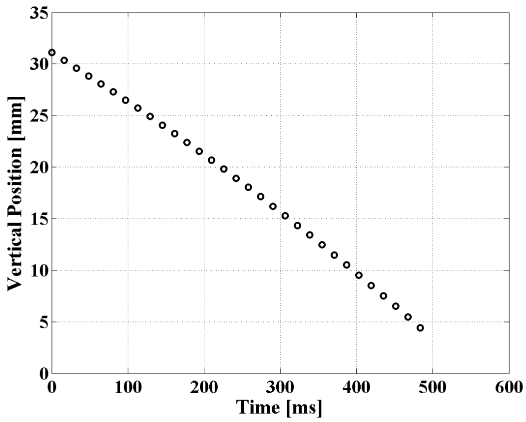

Figure 5: Droplet position as a function of time for a falling n-hexadecane droplet.

their diameter change due to the change in the distance between droplet and objective. In evaluating the images for determining the position, the refractive index and the size, this has been taken into account. In order to demonstrate that the results are correct, n-hexadecane droplets have been used. As n-hexadecane has a very low evaporation rate, droplet velocity, refractive index and size should remain almost constant. In Fig. 5 the vertical position is shown as a function of time, showing an almost constant falling velocity of $0.055\,\mathrm{m/s}$ of the droplet.

In Figs. 6 and 7 the refractive index and the droplet size respectively are shown as a function of time. It can clearly be seen that the refractive index as well as the droplet size remain constant as expected.

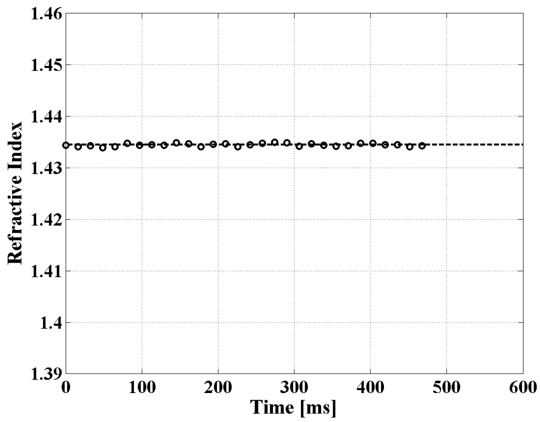

Figure 6: Refractive index as a function of time for a falling n-hexadecane droplet. Dashed line represents the expected value for the pure substance at 293.15 K.

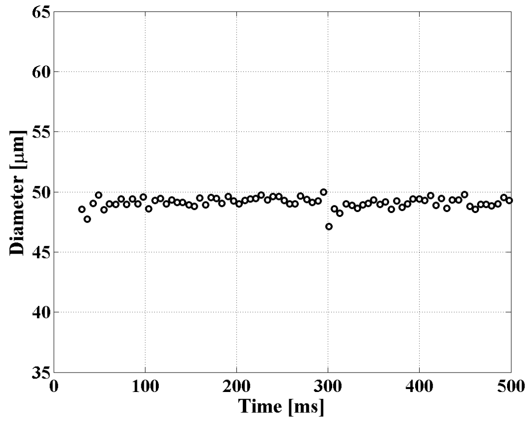

Figure 7: Droplet size as a function of time for a falling n-hexadecane droplet.

The refractive index has been obtained using rainbow signals (see Fig. 3) for each frame taken by the planar CCD-camera, which are compared with calculations of the rainbow signal using Nussenzveig's theory. For the size needed for the calculation of the theoretical signal the measured size has been used. Then from a large data base of theoretical signals with different refractive indices the one which fits best with the measured signal has been selected. Thus the correct refractive index is found. This is according to the method described in (7). The theoretical values considered for comparison have been calculated using the method suggested by (2) for a reference temperature of 293.15 K.

The droplet size has been obtained using the method described in (3).

Results for two droplets in the observation chamber are presented in the next section.

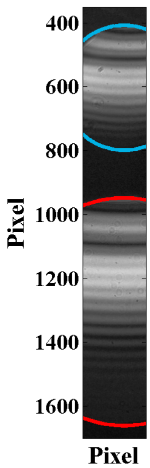

Figure 8: Image of the planar CCD-camera with the scattered light in the rainbow region of two droplets. The red lines indicate a n-decane droplet, the blue lines indicate a n-hexadecane droplet.

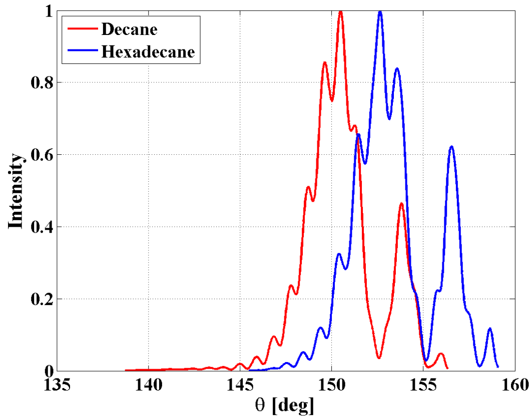

Figure 9: Rainbow signals obtained from Fig.8.

Results

In this section results for two droplets of different liquids and different size falling simultaneously but with slightly different terminal falling velocity in the observation chamber are presented.

For this purpose two droplet on demand generators are used. They are triggered in such a way, that the droplets are falling close one after the other along the illuminating laser beam. However, the distance must be large enough in order to omit an overlap of the signals. An image of the planar CCD-camera is shown in Fig. 8.

The red lines indicate a n-decane droplet, the blue lines indicate a n-hexadecane droplet. The corresponding rainbow signals are shown in Fig. 9. Now the different rainbow positions caused by the different refractive indices of the substances can be seen clearly. A series of images of the planar CCD-camera is shown in Fig. 10. In Fig. 11 the droplet positions as a function of time for the n-decane and the n-hexadecane droplets are shown. The velocity of the larger n-decane droplet is higher, resulting in an increasing distance between the droplets.

From the images of Fig. 10 the refractive indices are obtained as a function of time for both droplets. The results are shown in Fig. 12. The different refractive indices can be detected, however, no essential change with time can be measured for both liquids.

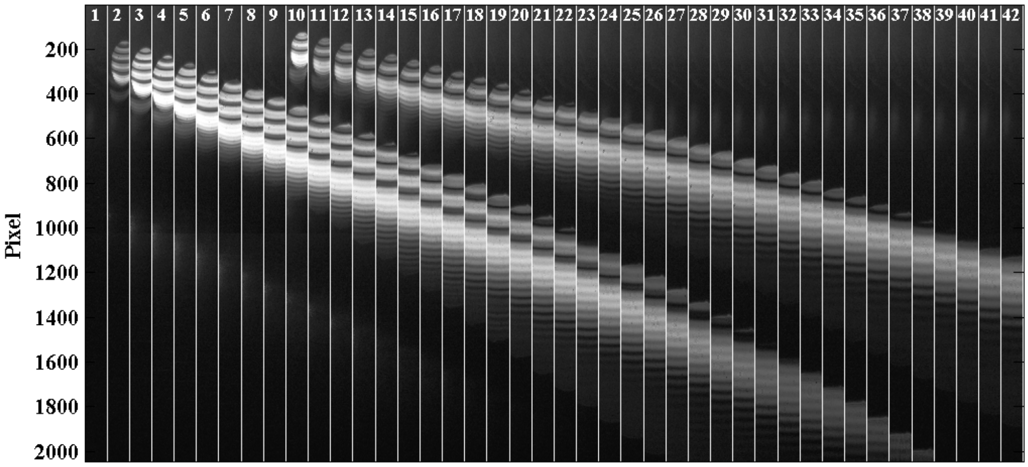

Figure 10: Series of grabbed images of the planar CCD-camara. The scattered light of two different droplets can be seen.

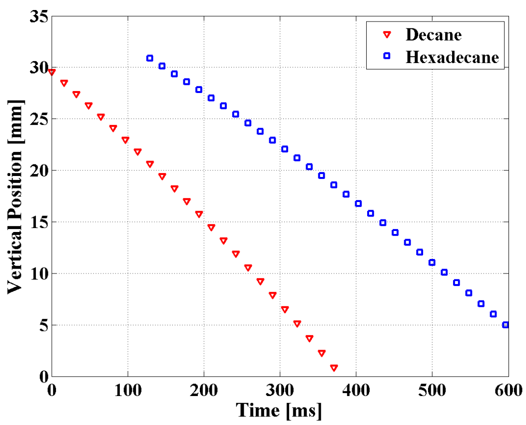

Figure 11: Droplet position as a function of time for a falling n-decane and a n-hexadecane droplet.

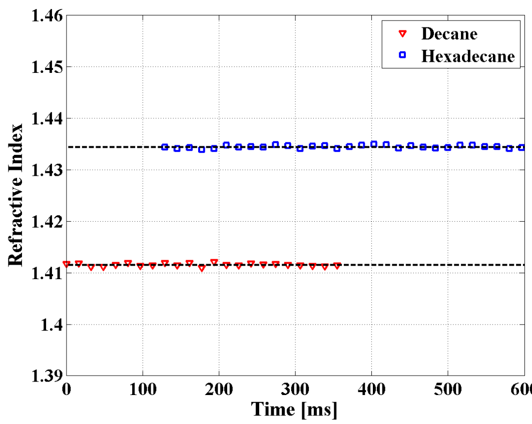

Figure 12: Refractive index as a function of time for two droplets simultaneously falling in the observation chamber. Dashed lines represent the expected value for the pure substances at 293.15 K.

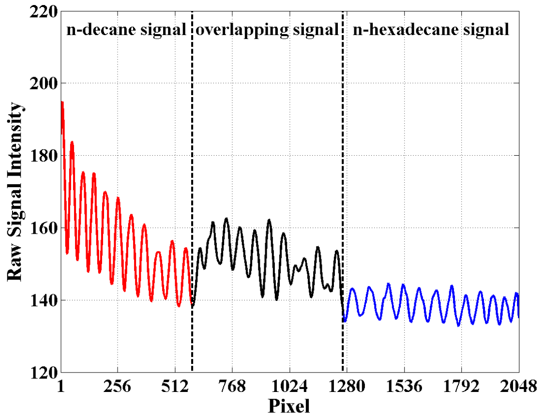

Figure 13: Smoothed signal obtained from the linear CCD-camera.

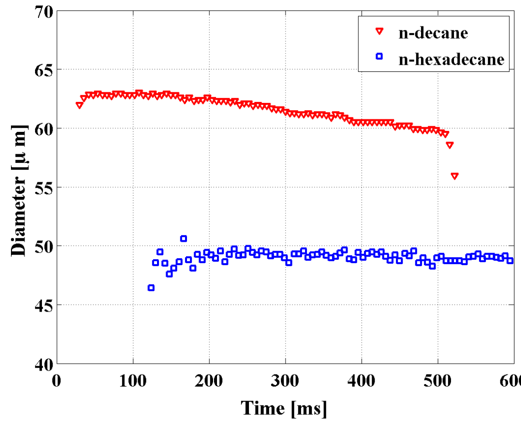

Figure 14: Droplet size as a function of time for two different droplets.

In Fig. 13 a processed signal of the linear CCD-camera grabbing the scattered light in the forward hemisphere is presented.

The signal of the two droplets is partly overlapping, nevertheless, for each droplet the size can be determined. Results of the evolution of the droplet sizes with time are shown in Fig. 14. The decrease in size of the n-decane droplet with the higher evaporation rate can be detected. However, only for a short time period both droplet sizes can be detected simultaneously. In order to enlarge this time period the optical setup has to be changed and the laser power has to be increased. This will be an issue for future investigations.

As can be seen from Fig. 11 the larger n-decane droplet falls with a higher velocity and the distance between the droplets increases. In the case the droplet generators are triggered in such a way that the larger droplet is falling behind the smaller one, collision of the droplets may occur in the observation region of the camera if the initial distance is small enough. Such a situation can be seen in Fig. 15.

The images before frame number twelve, which are frames before the droplet collision, show overlapping rainbow signals of the two droplets. The droplets have there a different but similar velocity. After frame number twelve it can clearly be seen, that the change in droplet position is larger from frame to frame, indicating the higher velocity of the larger droplet after collision. An enlarged view of the images just before and after frame number twelve is shown in Fig. 16. Here it can be seen, that the scattered light shown on frame number twelve is totally disturbed. This is a hint, that there the collision occurs and the new droplet is not spherical yet. Signals obtained from different frames around frame number twelve are shown in Figs. 17 to 20.

Figure 17 shows two overlapping rainbow signals. The signal of Fig. 18 may derive from an unspherical or very inhomogenous droplet during the mixing process.

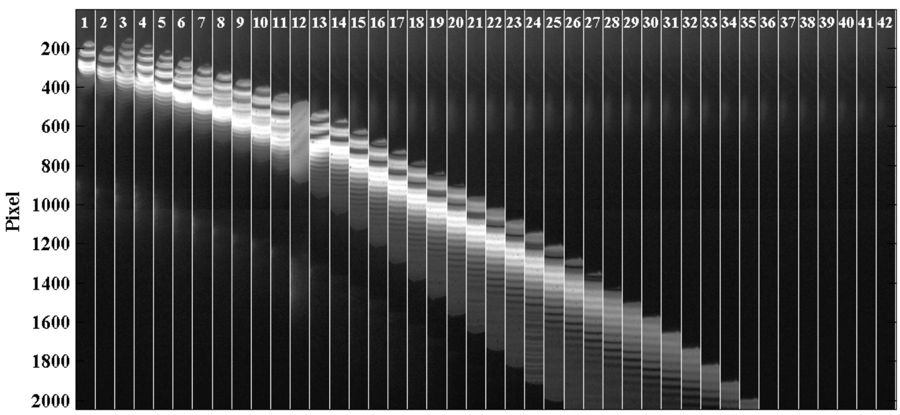

Figure 15: Series of images of the planar CCD-camera showing the scattered light of two colliding droplets.

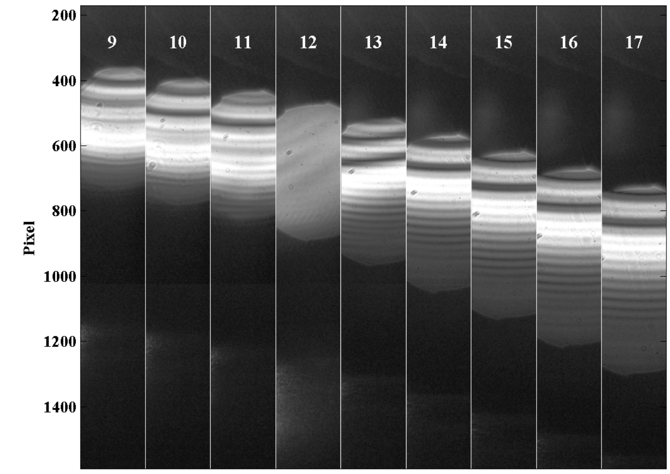

Figure 16: Series of images of the planar CCD-camera showing the scattered light of two colliding droplets (enlarged view of Fig. 15).

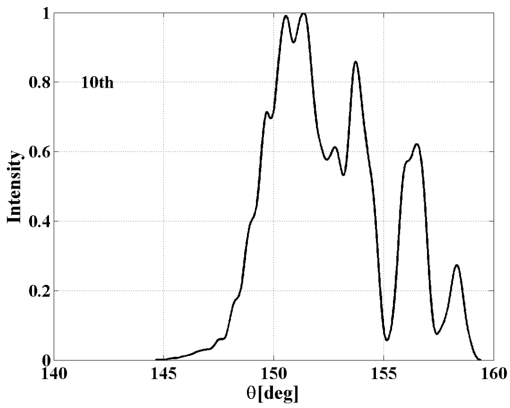

Figure 17: Signal obtained from frame 10

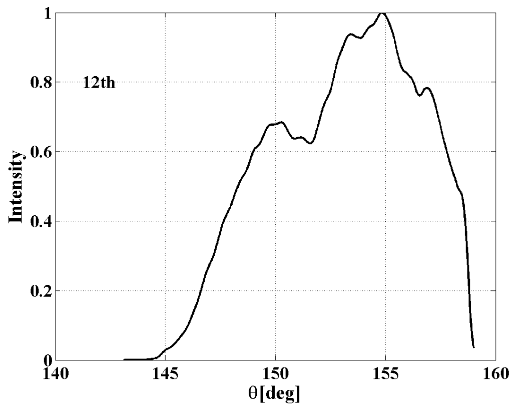

Figure 18: Signal obtained from frame 12

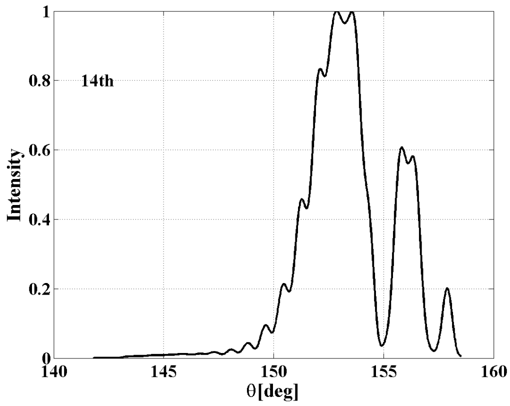

Figure 19: Signal obtained from frame 14

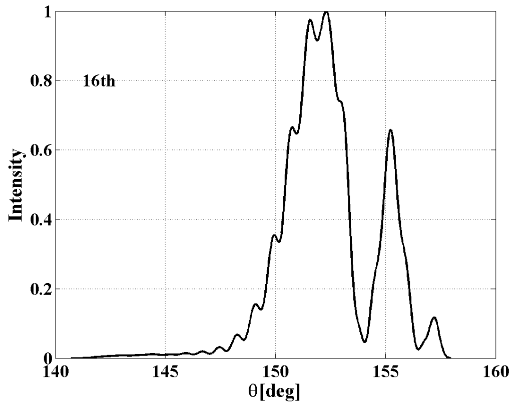

Figure 20: Signal obtained from frame 16

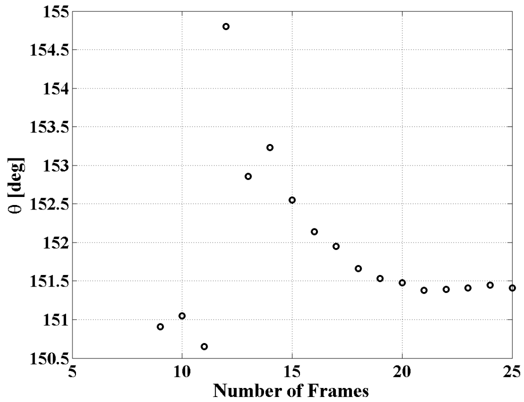

Figure 21: Position of the maxima obtained from the rainbow signal before and after the mixing process.

Both other images shown in Figs. 19 and 20 seem to characterize the droplet after the mixing process. In Fig. 21 the positions of the maxima derived from signals shown in the previous figures are shown for frames before and after the mixing process. According to Fig. 16 the collision process seems to start at frame number twelve and according to Fig. 21 it seems to be completed within frame thirty. These results show, that it may be possible to determine the duration of such mixing processes. However, still future work is needed in order to find out how to interprete and evaluate these results in detail.

Summary and Conclusions

In this paper an experimental method is presented to study two droplets freely falling in an observation chamber. It has been shown, that the velocities, sizes, and refractive indices of both droplets can be determined simultaneously. The experimental method may be a first step to extend the ILIDS or IMI technique for inverstigation of the rainbow. If this technique works in future refractive index measurements in a spray may be possible. Good results are expected for the study of the mixing of two sprays with different sprayed liquids, as the refractive indices differ a lot. The results show that even mixture processes may be studied in future. In future work improvements of the expermental setup will be performed, allowing then to study droplets with a closer distance. One focus of the investigations will then be the study of the mixing process. Another focus will be on the study of multicomponent droplets.

References

[1] N. Roth, J. Wilms, and B. Weigand. Technique for measurements of the evaporation rate of single, freely falling, droplets. In *Proc. 12th Int. Symp. on Application of Laser Techniques to Fluid Mechanics*, Vol. 1, Lisbon, Portugal, 2004.

[2] J. Wilms. *Evaporation of Multicomponent Droplets*. PhD Thesis, Universität Stuttgart, Verlag Dr. Hut, 2005. ISBN 3-89963-255-9.

[3] G. König, K. Anders, and A. Frohn. A new light-scattering technique to measure the diameter of periodically generated moving droplets. *J. Aerosol Sci.*, Vol. 17, pp. 157–167, 1986.

[4] T. Kobayashi, T. Kawaguchi, and M. Maeda. Measurement of spray flow by an improved interferometric laser imaging droplet sizing (ilids) system. In *10th. Int. Symp. Applications of Laser Techniques to Fluid Mechanics*, pp. 10.2, Lisbon, 2000.

[5] N. Damaschke, H. Nobach, T.I. Nonn, N Semidetonv, and C. A Tropea. Multi-dimensional particle sizing techniques. *Experiments in Fluids*, Vol. 39, No. 2, pp. 336–350,, 2005. DOI: 10.1007/s00348-005-1009-1.

[6] N. Roth. *Bestimmung des Brechungsindex in Einzeltropfen aus dem Streulicht im Bereich des Regenbogens*. PhD Thesis, University of Stuttgart, 1998. Verlag Shaker, Aachen.

[7] S. Saengkaew. *Development of Novel Global Rainbow Technique for Characterizing Spray Generated by Ultrasonic Nozzle*. PhD thesis, Chulancongkorn University, 2005. Department of Chemical Engineering, Faculty of Engineering.